

Non-monotonic magnetic field and density dependence of in-plane magnetoresistance in dilute two-dimensional holes in GaAs/AlGaAs

H. Noh, Jongsoo Yoon,* D. C. Tsui, and M. Shayegan

Department of Electrical Engineering, Princeton University, Princeton, NJ 08544

(April 26, 2024)

We studied low temperature ($T = 50\text{mK}$) in-plane magnetoresistance of a dilute two-dimensional hole system in GaAs/AlGaAs heterostructure that exhibits an apparent metal-insulator transition. We found an anisotropic magnetoresistance, which changes dramatically at high in-plane fields ($B_{\parallel} \gtrsim 5\text{T}$) as the hole density is varied. At high densities where the system behaves metallic at $B_{\parallel} = 0$, the transverse magnetoresistance is larger than the longitudinal magnetoresistance. With decreasing the hole density the difference becomes progressively smaller, and at densities near the "critical" density and lower, the longitudinal magnetoresistance becomes larger than the transverse magnetoresistance.

73.40.-c,73.40.Kp,71.30.+h,73.50.Jt

The scaling theory of localization¹ predicts that, in the absence of electron-electron interaction, all states in two dimensions (2D) are localized in the zero temperature limit and that only an insulating behavior characterized by an increasing resistivity (ρ) with decreasing temperature (T) is possible at low T . In contrast, experimental observations of a "metallic" behavior, characterized by a decreasing ρ with decreasing T , and thus an apparent metal-insulator transition (MIT) as charge carrier density is lowered, are reported on many different low disorder dilute 2D systems at low temperatures.² To date, despite the large number of experimental as well as theoretical papers in the literature, there is still no consensus on either the physics and the mechanism behind the metallic-like behavior or the origin of this apparent MIT.

From the more recent experiments, two factors that strongly influence the charge transport close to this MIT in these low density high mobility 2D systems have emerged. First, disorder is found to play a significant role. A close examination of all such 2D systems reveals that the critical density (n_c for electrons and p_c for holes), the density above which the system shows the metallic behavior, is lower in a system with higher carrier mobility. The two most extensively studied systems are the electron inversion layer in Si-MOSFET³ and the 2D holes in the GaAs/AlGaAs heterostructure.^{4,5} Typically, the 2D electrons in a high quality Si-MOSFET have a peak mobility of $\sim 2 \times 10^4 \text{cm}^2/\text{Vs}$ to $5 \times 10^4 \text{cm}^2/\text{Vs}$, and $n_c \sim 1 \times 10^{11} \text{cm}^{-2}$. In the extremely high mobility 2D hole system (2DHS) in GaAs/AlGaAs, which has a comparable effective mass at low densities and a more than 10 times higher peak mobility of $\sim 7 \times 10^5 \text{cm}^2/\text{Vs}$, $p_c \sim 1 \times 10^{10} \text{cm}^{-2}$. Both n_c and p_c are found to decrease with decreasing disorder in the 2D system,⁵ approaching the critical density characterized by the dimensionless density parameter $r_s = 37$, expected for Wigner crystallization in 2D.⁶

The second factor is the effect of a magnetic field applied parallel to the 2D plane. The parallel field (B_{\parallel}) is found to suppress the metallic behavior and also induce an unexpectedly large positive magnetoresistance

(MR). In the case of the 2DHS in GaAs,⁷ this giant MR follows $\sim \exp(B_{\parallel}^2)$ at low B_{\parallel} and crosses into an $\sim \exp(B_{\parallel})$ dependence at high B_{\parallel} around a well defined characteristic field B^* , which is hole density dependent. This behavior persists into the insulating phase, though B^* becomes density independent. Similarly strong positive MR was observed earlier in the electron inversion layer in Si-MOSFET's at low B_{\parallel} though it is followed by saturation⁸ or in some cases a weak linear dependence at high B_{\parallel} .

Recently, Das Sarma and Hwang⁹ pointed out the importance of taking into account in the B_{\parallel} transport the finite thickness of the 2D electrons through which B_{\parallel} can be coupled into their orbital motion. They calculated the Boltzmann transport in the presence of B_{\parallel} assuming δ -function random impurity scattering and a harmonic confinement of the 2D carriers to the heterojunction interface. They were able to produce a giant positive MR showing B_{\parallel} dependencies in qualitative agreement with experimental observations. In particular, their calculation showed almost two orders of magnitude increase in resistance, when B_{\parallel} was increased to 10T. Furthermore, they found a crossover from a low field to high field behavior due to the change of the relative magnitude of the cyclotron energy to the confinement energy with increasing field. The difference between the B_{\parallel} behavior seen in the Si inversion layer and that in the 2DHS in GaAs in the high field regime was attributed to the different impurity scattering mechanisms. Most importantly for experiments, they predicted that this giant in-plane MR is highly anisotropic: the transverse MR (ρ_{\perp} , the MR when $B_{\parallel} \perp I$, where I is the current) can be many times larger than the longitudinal MR (ρ_{\parallel} , the MR when $B_{\parallel} \parallel I$) for a moderately high B_{\parallel} in the 10T range.

In the course of a systematic study on the nature of the insulating ground state in the extreme dilute limit of the 2DHS in GaAs, we have investigated the B_{\parallel} transport in one of the highest mobility low density sample currently available as a function of the hole density (p) across the apparent MIT with B_{\parallel} up to 14T at dilution

refrigerator temperatures down to 50mK. By exploring a regime (lower density, lower temperature) not accessible in previous in-plane MR anisotropy experiments, we find a behavior which cannot be understood with currently available models. In addition to observing the expected behavior of a much larger MR in this regime, we find that the anisotropy, defined as the difference between ρ_{\parallel} and ρ_{\perp} , changes sign in the high field region as the hole density is decreased. For densities $p > 2 \times 10^{10} \text{cm}^{-2}$, ρ_{\perp} is larger than ρ_{\parallel} at high field similar to the model calculation by Das Sarma and Hwang. However, the difference between ρ_{\perp} and ρ_{\parallel} becomes progressively smaller as the density is decreased, and for densities $p < 2 \times 10^{10} \text{cm}^{-2}$, ρ_{\parallel} becomes larger than ρ_{\perp} . In the rest of this paper, we describe in more detail the experiment and discuss our data in light of more recent results from ^3He temperature experiments in the metallic regime.¹⁰ We also point out that the observed anisotropy is at variance with predictions of existing theories explaining the large in-plane MR.

Our samples are made from a modulation doped GaAs/AlGaAs (311)A single interface heterostructure grown by molecular beam epitaxy. The 2DHS at the (311)A interface even at $B_{\parallel} = 0$ exhibits a mobility anisotropy known to be due to anisotropic surface morphology.¹¹ The mobility is high along the [233] crystallographic direction, and low along the [01 $\bar{1}$] direction. We made two Hall bar (rectangular) samples, one for each direction, from the same wafer. For resistivity measurements, I was always passed along the sample length. Both samples also have back gates to change their density. The peak mobilities at $T = 50\text{mK}$ for our ungated samples with a density of $p = 4.2 \times 10^{10} \text{cm}^{-2}$ are $6.3 \times 10^5 \text{cm}^2/\text{Vs}$ along [233] and $4.2 \times 10^5 \text{cm}^2/\text{Vs}$ along [01 $\bar{1}$]. These are among the highest mobilities achieved in samples of this type of single interface heterostructures. Our measurements were made down to $p = 7.9 \times 10^9 \text{cm}^{-2}$. This density is about 40% lower than that accessed by Papadakis *et al.* in their recent experiments using the GaAs/AlGaAs (311)A quantum wells at ^3He temperatures.¹⁰ It enabled us to measure the in-plane MR across the zero-field MIT at $p_c = 9.3 \times 10^9 \text{cm}^{-2}$. For a given density, we measured both $\rho_{\perp}(B_{\parallel})$ and $\rho_{\parallel}(B_{\parallel})$ by applying B_{\parallel} up to 14T. The samples were mounted, in separate cooldowns, on a rotating stage in a dilution refrigerator, which could adjust the angle between the 2D plane and the direction of the magnetic field. They were mounted in such a way that either $B_{\parallel} \perp I$ for ρ_{\perp} measurement or $B_{\parallel} \parallel I$ for ρ_{\parallel} measurement, when the 2D plane is aligned parallel to the magnetic field. Between the ρ_{\perp} and ρ_{\parallel} measurements, the samples were thermally recycled, and measurements were repeated for consistency check.

The in-plane MR, $\rho_{\perp}(B_{\parallel})$ and $\rho_{\parallel}(B_{\parallel})$, measured at 50mK for I fixed in [233] direction are shown in Fig. 1 (a) and (b), respectively, in the density range from $4.25 \times 10^{10} \text{cm}^{-2}$ to $0.79 \times 10^{10} \text{cm}^{-2}$. The sample shows insulating

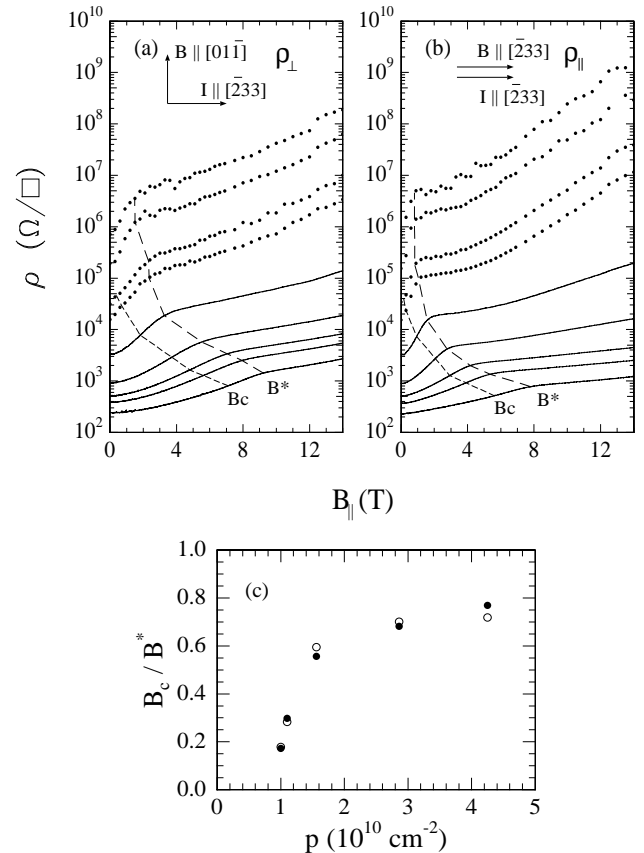


FIG. 1. (a) ρ_{\perp} and (b) ρ_{\parallel} plotted as a function of B_{\parallel} at densities $p = 4.25, 3.25, 2.86, 2.18, 1.56, 1.10, 1.00, 0.87, 0.79 \times 10^{10} \text{cm}^{-2}$ (from bottom to top). The critical density p_c , where the MIT occurs at zero-field, is $p_c = 0.93 \times 10^{10} \text{cm}^{-2}$. The characteristic field B_c , above which the metallic behavior is suppressed, is marked by the short dashed line, and B^* , which divides the low field and the high field regions, is marked by the long dashed line. The orientation of B_{\parallel} and I are shown with respect to the crystal axes. In both (a) and (b), the solid lines are data measured by low frequency lock-in technique and the solid circles are those measured by DC I-V measurement. (c) B_c/B^* plotted as a function of p . Solid (open) symbols are for $B_{\parallel} \perp I$ ($B_{\parallel} \parallel I$).

behavior at $B_{\parallel} = 0$ for the two lowest densities (the top two traces) and metallic behavior for the higher densities. Both ρ_{\perp} and ρ_{\parallel} show strong increase with increasing B_{\parallel} , about one order of magnitude for the highest density and more than two (ρ_{\perp}) or three (ρ_{\parallel}) orders of magnitude for the lowest density at 14T. It is clear that the MR is larger for lower densities. We should also note that the MR in our sample is approximately ten times larger than that observed by Papadakis *et al.*¹⁰ at $T = 0.3\text{K}$ in the density range where the two experiments overlap.

For both ρ_{\perp} and ρ_{\parallel} , according to their dependence on B_{\parallel} , the ρ - B_{\parallel} plane can be divided into two regions: a low field region ($B_{\parallel} < B^*$) and a high field region ($B_{\parallel} > B^*$). In the low field region, ρ measured in both

field orientations increases rapidly with increasing B_{\parallel} , following $\rho \sim \exp(B_{\parallel}^2)$. This rapid increase slows down as B_{\parallel} is increased to the high field region, where ρ_{\perp} increases as $\exp(B_{\parallel})$, while ρ_{\parallel} shows a behavior depending on the density. For densities $p > 2.18 \times 10^{10} \text{cm}^{-2}$, ρ_{\parallel} also increases as $\exp(B_{\parallel})$, but for lower densities, it shows a stronger dependence, which becomes more pronounced when the density is lowered. For both B_{\parallel} orientations, the metallic behavior observed at $B_{\parallel} = 0$ and $p > p_c$ is suppressed for $B_{\parallel} > B_c$ (the short dashed lines in Fig. 1 (a) and (b)). Both B_c and B^* are smaller in Fig. 1 (b) than in Fig. 1 (a). However, as shown in Fig. 1 (c), when the ratio of B_c to B^* is plotted as a function of p , the two sets of data are nearly identical. These observations result from a B_{\parallel} induced spin subband depopulation identified recently by Papadakis *et al.*¹⁰ and Tutuc *et al.*¹² from their detailed analyses of the Shubnikov-de Haas oscillations observed at 0.3K. We shall later return to this point.

In Fig. 2 (a), we plot both $\rho_{\perp}(B_{\parallel})$ and $\rho_{\parallel}(B_{\parallel})$ from Fig. 1 normalized by the values at $B_{\parallel} = 0$ in a single plot to show the anisotropy. Note that in Fig. 2 (a) both sets of data were taken with I fixed along $[2\bar{3}3]$ and the direction of B_{\parallel} was varied from $[01\bar{1}]$ to $[2\bar{3}3]$ to measure ρ_{\perp} and ρ_{\parallel} , respectively. In Fig. 2 (b), we show additional data, taken with I along $[01\bar{1}]$ and B_{\parallel} along $[2\bar{3}3]$ (ρ_{\perp}), and compare them with ρ_{\parallel} of Fig. 2 (a), which is taken with both I and B_{\parallel} along $[2\bar{3}3]$. In other words, in Fig. 2 (b) the direction of B_{\parallel} is fixed along $[2\bar{3}3]$, and ρ_{\perp} and ρ_{\parallel} data are shown for I along $[01\bar{1}]$ and $[2\bar{3}3]$, respectively. The data of Fig. 2 highlight the central finding of our paper: *in the high field region, on the right of the dotted lines, we observe an anisotropy in MR which reverses sign as a function of density.* At high densities ρ_{\perp} is larger than ρ_{\parallel} , while at low densities ρ_{\parallel} is larger than ρ_{\perp} . This $\rho_{\parallel} > \rho_{\perp}$ anisotropy continues to grow across the MIT, and for $p \lesssim p_c$, in the $B_{\parallel} = 0$ insulating side, ρ_{\parallel} is approximately an order of magnitude larger than ρ_{\perp} at 14T. Note that this trend is seen regardless of whether ρ_{\perp} and ρ_{\parallel} are measured by fixing the direction of I (Fig. 2 (a)) or B_{\parallel} (Fig. 2 (b)), suggesting that the relative orientation of I and B_{\parallel} is important in the high field region. No change of anisotropy at high field with decreasing density was observed in earlier $T = 0.3\text{K}$ experiments,¹⁰ where a relatively high density sample, showing only the metallic behavior at $B_{\parallel} = 0$, was studied. There, ρ_{\perp} was always larger than ρ_{\parallel} even at B_{\parallel} up to 16T. Before we further discuss this surprising trend, it is useful to make a few remarks about the MR data at lower B_{\parallel} , on the left of the dotted lines in Fig. 2.

As mentioned before, each of our MR traces has a characteristic field, B^* . It has been recently shown that B^* marks the field above which the 2DHS becomes fully spin polarized.^{10,12,13} Below B^* , two spin subbands with unequal populations are occupied while, above B^* , there is only one occupied spin subband. The situation is similar for 2D electron systems in Si-MOSFET's; there too a

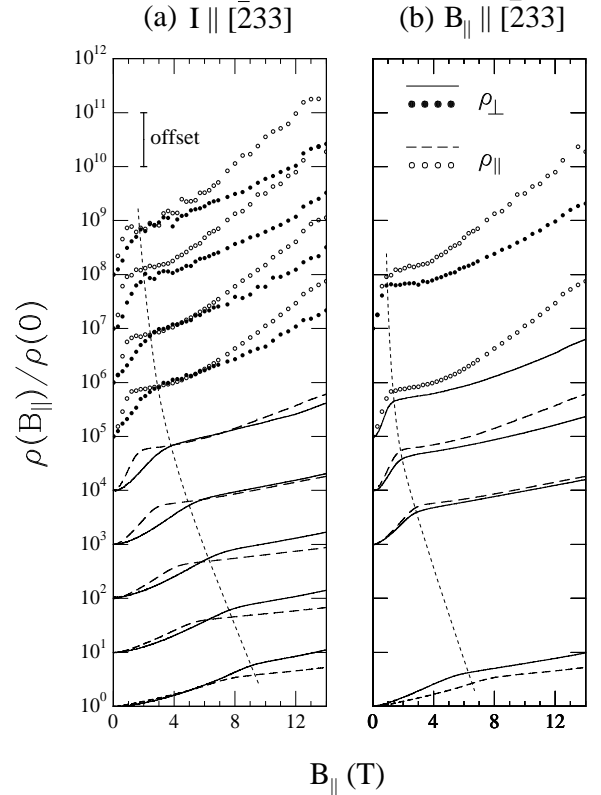


FIG. 2. ρ_{\perp} and ρ_{\parallel} normalized by the zero-field resistivity $\rho(0)$ and plotted together for (a) I fixed along $[2\bar{3}3]$ and (b) B_{\parallel} fixed along $[2\bar{3}3]$. The solid lines and solid circles are for ρ_{\perp} and the dashed lines and open circles are for ρ_{\parallel} . The densities for each pair of traces in (a) from bottom to top is $p = 4.25, 3.25, 2.86, 2.18, 1.56, 1.10, 1.00, 0.87, 0.79 \times 10^{10} \text{cm}^{-2}$. The data for each p are offset by 10 as indicated by the scale bar for clarity. The densities in (b) from bottom to top is $p = 4.25, 2.18, 1.56, 1.10, 0.87 \times 10^{10} \text{cm}^{-2}$ and the data are offset in such a way that zero-field values match with those in (a) for corresponding densities. The dotted lines are guide to the eye, representing the boundary between the low and high field regions.

strong MR is observed at low fields when two spin subbands are populated, while the MR is essentially saturated once the system is fully spin polarized.^{14,15} Calculations by Dolgoplov *et al.*¹⁶ and Herbut¹⁷ attribute this low field MR to the change of screening as the spin polarization changes. In the case of 2DHS in GaAs (311)A, B^* depends on the orientation of the B_{\parallel} with respect to the crystal axes. In particular, B^* is smaller for $B_{\parallel} \parallel [2\bar{3}3]$ compared to $B_{\parallel} \parallel [01\bar{1}]$. This is due to the intrinsic energy band anisotropy of the GaAs (311)A 2DHS, as has been documented experimentally and theoretically.^{10,12,13} Our observation that B^* in the ρ_{\perp} data of Fig. 1 (a) is larger than in the ρ_{\parallel} data of Fig. 1 (b) is consistent with these findings. That the data plotted as B_c/B^* for the two B_{\parallel} orientations in Fig. 1 (c) should closely agree is also to be expected if the minority spin population is constant at

B_c as found by Tutuc *et al.*¹² and the spin polarization is linear in B_{\parallel} .

It is likely that the MR anisotropy observed at low fields in Fig. 2 (a) is a consequence of the difference in spin subband depopulation rate for different orientations of B_{\parallel} with respect to the crystal axes. An alternative interpretation of the low field anisotropy may be based on a recent theory by Chen *et al.*¹⁸ These authors find that an interplay between the spin-orbit coupling and the Zeeman splitting can lead to an anisotropic MR depending on the relative direction between I and B_{\parallel} . The anisotropy is small at low and high fields, and exhibits a maximum at an intermediate field when the Zeeman energy equals the spin-orbit induced spin-splitting. At first sight, this seems qualitatively consistent with the low field portion of Fig. 2 (a) where the difference between ρ_{\parallel} and ρ_{\perp} goes through a maximum. However, this trend is not observed in Fig. 2 (b) which also compares ρ_{\parallel} and ρ_{\perp} but now for a fixed B_{\parallel} direction. We conclude that the explanation of the anisotropic MR observed in the low field region in Fig. 2 (a) most likely lies in the anisotropic spin subband depopulation.¹⁰

We now return to a discussion of the high field data which are the main subject of this paper. We first note that these data are in a field region where only one spin subband is occupied and the system is fully spin polarized. In this region, calculations such as those reported in Refs. 16 and 17 predict that the MR would saturate. A saturation of the MR above B^* is indeed often seen in 2D electron systems in Si-MOSFET's.^{14,15} This is in contrast, however, with the data shown in Fig. 2 where a large MR is observed even at high fields beyond B^* . Calculations by Das Sarma and Hwang,⁹ on the other hand, point to the coupling of B_{\parallel} to the orbital motion, and show that there can be a significant MR when the magnetic length becomes comparable to or smaller than the layer thickness. They also predict that the MR should be anisotropic with $\rho_{\perp} > \rho_{\parallel}$. While this trend is seen in our data at high densities (Fig. 2), the anisotropy is reversed at low densities. Their calculations predict that with decreasing density, the anisotropy ($\rho_{\perp} > \rho_{\parallel}$) increases because of the increasing layer thickness. This is also at odds with our experimental data, although we should note that in our samples we expect the layer thickness to decrease with decreasing density since we are using a back gate. It is remarkable that the low density data indicate that at high fields $\rho_{\parallel} > \rho_{\perp}$ regardless of whether the direction of I or B_{\parallel} is kept fixed. This observation suggests that the anomalous anisotropy we observe at low densities may be intrinsic to very dilute 2D hole systems in GaAs.

Finally, Meir¹⁹ explained the large in-plane MR in GaAs as from inhomogeneous distribution of charge carriers due to disorder. In his model, the disorder potential induces puddles of 2D holes which are interconnected by quantum point contacts (QPC), and the transport is dominated by the conduction through these QPC's. An in-plane magnetic field increases the bottom of the 2D

subbands and effectively increases the conduction threshold energy of the QPC's, giving rise to the large positive MR. The MIT is a percolation transition which can be tuned by density and by in-plane magnetic field because the conduction through the QPC's depends on the relative value of the Fermi energy to the threshold energy of the QPC's. However, no anisotropy is expected in this model, where the MR arises from the shift of the 2D subband energy by the presence of B_{\parallel} .

In summary, we have measured the in-plane MR ρ_{\perp} and ρ_{\parallel} of a very high mobility, dilute 2DHS in the GaAs/AlGaAs heterostructure in the density range from $4.2 \times 10^{10} \text{cm}^{-2}$ to $7.9 \times 10^9 \text{cm}^{-2}$, spanning across the apparent zero-field MIT. In the low B_{\parallel} region, the observed anisotropy is consistent with the spin subband depopulation which depends on the orientation of B_{\parallel} relative to the crystal axes. In the high field region, we observed a change in the sign of the anisotropy with decreasing density. At high densities, $\rho_{\perp} > \rho_{\parallel}$. However, as the density is lowered, this anisotropy decreases and ρ_{\parallel} becomes equal to ρ_{\perp} around $\sim 2 \times 10^{10} \text{cm}^{-2}$. For still lower densities, $\rho_{\parallel} > \rho_{\perp}$, and the anisotropy changes sign and also grows continuously across the MIT. These experimental observations are not explicable with existing theoretical models for the in-plane MR.

We would like to thank S. Das Sarma, E. H. Hwang, Y. Meir, P. Phillips, and M. Hilke for fruitful discussions. This work was supported by the NSF.

* Present address: Department of Physics, University of California, Berkeley, CA 94720.

- ¹ E. Abrahams, P. W. Anderson, D. C. Licciardello, and T. V. Ramakrishnan, *Phys. Rev. Lett.* **42**, 673 (1979).
- ² For a review, see E. Abrahams, S. V. Kravchenko, M. P. Sarachik, *Rev. Mod. Phys.* **73**, 251 (2001).
- ³ S. V. Kravchenko *et al.*, *Phys. Rev. B* **50**, 8039 (1994); D. Popović *et al.*, *Phys. Rev. Lett.* **79**, 1543 (1997); V. M. Pudalov, *JETP Lett.* **66**, 175 (1997).
- ⁴ Y. Hanein *et al.*, *Phys. Rev. Lett.* **80**, 1288 (1998); M. Y. Simmons *et al.*, *Phys. Rev. Lett.* **80**, 1292 (1998); A. P. Mills, Jr. *et al.*, *Phys. Rev. Lett.* **83**, 2805 (1999).
- ⁵ J. Yoon *et al.*, *Phys. Rev. Lett.* **82**, 1744 (1999).
- ⁶ B. Tanatar and D. M. Ceperley, *Phys. Rev. B* **39**, 5005 (1989).
- ⁷ J. Yoon *et al.*, *Phys. Rev. Lett.* **84**, 4421 (2000).
- ⁸ D. Simonian *et al.*, *Phys. Rev. Lett.* **79**, 2304 (1997).
- ⁹ S. Das Sarma and E. H. Hwang, *Phys. Rev. Lett.* **84**, 5596 (2000).
- ¹⁰ S. J. Papadakis *et al.*, *Phys. Rev. Lett.* **84**, 5592 (2000).
- ¹¹ J. J. Heremans *et al.*, *J. Appl. Phys.* **76**, 1980 (1994); M. Wassermeier *et al.*, *Phys. Rev. B* **51**, 14721 (1995).
- ¹² E. Tutuc *et al.*, *Phys. Rev. Lett.* **86**, 2858 (2001).
- ¹³ R. Winkler *et al.*, *Phys. Rev. Lett.* **85**, 4574 (2000).
- ¹⁴ T. Okamoto *et al.*, *Phys. Rev. Lett.* **82**, 3875 (1999).
- ¹⁵ S. A. Vitkalov *et al.*, *Phys. Rev. Lett.* **85**, 2164 (2000).
- ¹⁶ V. T. Dolgoplov and A. Gold, *JETP Lett.* **71**, 27 (2000).
- ¹⁷ I. F. Herbut, *Phys. Rev. B* **63**, 113102 (2001).
- ¹⁸ G.-H. Chen *et al.*, *Phys. Rev. B* **61**, 10539 (2000).
- ¹⁹ Y. Meir, *Phys. Rev. B* **61**, 16470 (2000).